Original Article

Improving sensitivity and imaging depth of ultrasound-switchable fluorescence via an EMCCD-gain-controlled system and a liposome-based contrast agent

Tingfeng Yao[1,2#], Yang Liu[1,2#], Liqin Ren[1,2], Baohong Yuan[1,2]

[1]Ultrasound and Optical Imaging Laboratory, Department of Bioengineering, The University of Texas at Arlington, Arlington, TX, USA; [2]Joint Biomedical Engineering Program, The University of Texas at Arlington and The University of Texas Southwestern Medical Center, Dallas, TX, USA

[#]These authors contributed equally to this work.

Correspondence to: Baohong Yuan. Department of Bioengineering, University of Texas at Arlington, Arlington, TX, USA. Email: baohong@uta.edu.

Background: The ultrasound-switchable fluorescence (USF) technique was recently developed to achieve high-resolution fluorescence imaging in centimeters-deep tissue. This study introduced strategies to significantly improve imaging sensitivity and depth using an electron multiplying charge-coupled device (EMCCD) camera-based USF imaging system and a newly developed USF contrast agent of indocyanine green (ICG)-encapsulated liposomes. For a quantitative study, a phantom of a sub-millimeter silicone tube embedded in centimeter-thick chicken breast tissue was adopted in this study as a model.

Methods: The synthesized ICG-liposome was characterized and compared with the previously reported ICG-nanogel. The exposure of the EMCCD camera was controlled via the MATLAB (The MathWorks, Inc. USA), instead of an external hardware trigger. The stability of the electron multiplying (EM) gain of the EMCCD camera was compared between two trigger modes: the MATLAB trigger mode and the external hardware trigger mode. The signal-to-noise ratio (SNR) of the USF imaging with different EM gain in various thick tissue was studied.

Results: The hydrodynamic size of the ICG-liposome was ~181 nm. The ICG-liposome had a sharper temperature switching curve and a better USF performance than the previously reported ICG-nanogel. The EM gain was more stable in MATLAB trigger mode than the external hardware trigger mode. Although, as usual, the SNR decreased quickly with the increase of the tissue thickness, the proposed strategies improved the SNR and the imaging depth significantly by adopting the novel contrast agent and controlling the EM gain.

Conclusions: We successfully imaged the sub-millimeter silicone tube with an inner diameter of 0.76 mm and an outer diameter of 1.65 mm in 5.5 cm-thick chicken breast tissue using 808 nm excitation light with a low intensity of 28.35 mW/cm^2, the improved EMCCD camera-based USF imaging system and the novel ICG-liposomes.

Keywords: Indocyanine green (ICG); liposome; near-infrared (NIR); ultrasound-switchable fluorescence (USF); high resolution; deep tissue imaging

Submitted Jun 25, 2020. Accepted for publication Sep 06, 2020.
doi: 10.21037/qims-20-796
View this article at: http://dx.doi.org/10.21037/qims-20-796

Introduction

Near infrared (NIR) fluorescence can penetrate biological tissue several centimeters via scattering, which enables deep tissue NIR fluorescence imaging. Unfortunately, it suffers from poor spatial resolution in centimeters-deep tissue because of tissue's high scattering property. In recent years, many researchers are interested in improving the spatial resolution of NIR fluorescence imaging in centimeter-deep tissues via various strategies, such as NIR-II fluorescence (1-4), ultrasound-pulse-guided digital phase conjugation (5), ultrasound-modulated fluorescence (6-10) and ultrasound-induced temperature-controlled fluorescence (11-14).

Adopting excitation and/or emission light at the NIR-II window (950–1,700 nm) can significantly reduce tissue's light scattering and has shown promising results in centimeter-deep tissues. For example, a study adopted 980 nm excitation light with strong intensity of ~300 mW/cm^2 and detected ~800 nm emission light (via upconversion) to image a 3.5 mL cuvette filled with core/shell nanoparticles and covered by a piece of 3.2 cm-thick porcine muscle tissue (3). Another study also used 980 nm excitation light with strong intensity of ~500 mW/cm^2 and ~1,100 nm emission light to image structures (a few millimeters) in a 6 cm-deep muscle tissue via a DOLPHIN imaging system (4). However, some concerns may exist when applying these methods for clinical uses: the biocompatibility and toxicity of the adopted NIR-II contrast agents, and potential significant heating effect of the high intensity excitation light (in order to obtain enough signal photons) on tissue due to the high absorption coefficient of water in tissues at NIR-II region.

During the past years, we developed a new imaging technique, ultrasound-switchable fluorescence (USF), to achieve high-resolution fluorescence imaging in centimeters-deep tissue (13-18). The ultrasound-switched-on fluorescence emission (via a thermal sensitive contrast agent) was confined within the ultrasound focal volume (or the ultrasound-induced thermal focal volume depending on the fluorescence detection time of the system) to obtain the fluorescence image with an ultrasound or ultrasound-scaled spatial resolution. Several indocyanine green (ICG) (an FDA approved fluorophore)-based USF contrast agents have been developed to take the advantage of the large penetration depth of the NIR-I photons (14,19-21). A β-cyclodextrin/ICG complex-encapsulated poly(N-isopropylacrylamide) (PNIPAM) nanogel (ICG-nanogel) was recently developed in our lab and USF imaging was successfully demonstrated *in vitro*, *ex vivo* and *in vivo* (20). It showed an improved signal-to-noise ratio (SNR) in USF imaging in a piece of 3.5 cm-thick chicken breast tissue compared with our previous ICG-based USF contrast agent (19). In this study, we will use this ICG-nanogel as a comparison. While this ICG-nanogel showed a promising USF performance, the adopted material of PNIPAM might generate a safety concern due to the potential toxicity of its monomers (NIPAM) to living cells. To address this concern, the biocompatible ICG-liposomes were recently developed in our lab by encapsulating the ICG dye into 1,2-dipalmitoylsn-glycero-3-phosphocholine (DPPC)-based liposomes. *In vitro*, *ex vivo* and *in vivo* USF images were successfully achieved using this novel contrast agent (21). However, one disadvantage of this 1st-generation ICG-liposome is its large hydrodynamic size (~7 μm), which is too large and limits its *in vivo* application. Therefore, reducing its size is highly desired. In this study, we reduced the hydrodynamic size of the ICG-liposome down to 181 nm, and its USF performance was found superior to that of the ICG-nanogel.

Recently, we demonstrated that an electron multiplying charge-coupled device (EMCCD) camera-based USF imaging system could well overcome the limitations of our previous USF imaging systems in which a single-fiber was used to collect photons to a photomultiplier tube, including the improved photon collection efficiency via the EMCCD camera and related lenses, and the increased imaging speed by adopting a Z-scan method (14,15,17). To apply the Z-scan method, the USF dynamic pattern was studied to determine the time interval and space interval between two sequential scan points to avoid signal interference induced by the thermal diffusion. However, the EM gain was observed to be unstable when recording a sequence of images after responding the external hardware trigger which was used to synchronize the camera with other devices (such as an ultrasound transducer and a translation stage). Therefore, the advantage of the EMCCD camera was not fully taken in our previous study in which an EM gain of 1 was adopted to achieve stable USF signals (20). However, to image much deeper tissue (such as >3 cm in chicken breast tissue), USF photons need to be significantly amplified so that they can clearly outstand from the background photons and be clearly differentiated from the noise caused by the background photons. To achieve this goal, a relatively stable gain is required. Therefore, instead of using the hardware trigger mode, in this study we adopted a software trigger mode by using MATLAB (The MathWorks, Inc. USA) to control

the software of the EMCCD camera (i.e., LightField from the manufacturer). This software trigger mode not only simplified the system but also reduced the temperature-induced EM gain variation. Our results showed this software trigger mode could provide a more stable gain compared with the hardware trigger mode. The SNRs of USF images with different EM gains in various thick tissues were also studied. By combining the improved ICG-liposome and the USF imaging system, we successfully achieved the USF imaging of a sub-millimeter silicone tube (inner diameter: 0.76 mm, outer diameter: 1.65 mm) embedded in 5.5 cm-thick chicken breast tissue using an excitation laser with a low intensity of 28.35 mW/cm^2.

Methods

ICG-liposome synthesis

The ICG-liposome was synthesized based on the previously reported method with modifications (21). First, the ICG solution was prepared by dissolving the ICG dye (Chem-Impex Int'L Inc., USA) in chloroform (99.9% pure) and ethanol mixture (4:1 v/v) at a concentration of 0.28 mg/mL. 5.0 mg DPPC (Avanti, USA) was dissolved with 2 mL chloroform in a 50 mL round flask and 0.2 mL of the prepared ICG solution was added later. After a well-mixing of the solution, the solvent was evaporated using a rotary evaporator (BUCHI Corp., USA) at 150 rpm with –80 kPa vacuum in a 55 ℃ water bath for at least 30 min to form a thin lipid layer on the wall of the round flask. Afterward, 0.8 mL hydration water, which was made by mixing 95 % PBS (pH 7.4) and 5 % glycerol (99.8% pure), was added into the flask and swirled at 55 ℃ for 1 min and then rotated for 1 hour at 150 rpm in a 42 ℃ water bath. Then, the ICG-liposome solution was vortexed using the amalgamator (DB338, Medical Instrument Co., Ltd, China) for 1 min. The obtained ICG-liposome was diluted to a final volume of 3.5 mL. Thus, theoretically, the maximum ICG concentration is 0.016 mg/mL (0.28 mg/mL × 0.2 mL/3.5 mL). A freeze-thaw-mix cycle was performed for 5 times by freezing the ICG-liposome in dry ice for 8 min and then transferred the ICG-liposome into a 60 ℃ water bath to thaw for 5 min followed by shaking the sample for 2 min with a shaker at 250 rpm. To control and uniform the size of liposome vesicles, an extrusion method was conducted with a mini-extruder (Avanti, USA). A 200 nm polycarbonate filter (Whatman, UK) was utilized and the ICG-liposome was extruded at 50 ℃ for 19 times. The obtained ICG-liposome was stored at 4 ℃. All chemicals were purchased from Fisher Scientific International, Inc., USA.

EMCCD-based USF imaging system

The schematic diagram of the proposed USF imaging system in this study is shown in *Figure 1A*. It was improved from the previously developed EMCCD-based USF imaging system (17). Briefly, the excitation laser with a wavelength of 808 nm (MGL-II-808-2W, Dragon lasers, China) was driven by the first function generator (FG1, 33500B, Agilent, USA). The output light was filtered by a bandpass filter (FF01-785/62-25, Semrock Inc., USA) and coupled into a dual branch light guide (1/4 × 72", Edmund Optics Inc., USA). To make uniform illumination, the tissue sample placed in a water tank was illuminated by the excitation light from two opposite directions. The emitted fluorescence from the contrast agents transmitted through two 2-inch longpass filters (BLP01-830R-50, Semrock Inc., USA), a camera lens (AF NIKKOR 50 mm f/1.8D Lens, Nikon, Japan), a 1-inch longpass filter (BLP01-830R-25, Semrock Inc., USA) and received by the EMCCD camera (ProEM®-HS:1024BX3, Princeton Instruments, USA) with a field of view around 4 cm × 4 cm (slightly variant when imaging different thick sample because of adjusting lens focus). The driving signal from the second function generator (FG2, 33500B, Keysight Technologies, USA) was amplified by a 50 dB-gain radio frequency power amplifier (RF-AMP, A075, E&I, USA), passed through a matching network and delivered to a 2.5 MHz high intensity focused ultrasound (HIFU) transducer (H-108, Sonic Concepts Inc., USA). To realize the sample scanning, the HIFU transducer was mounted to a three-axis motorized translation stage (XSlide™ and VXM™, Velmex Inc., USA). The temperature of the water was controlled at 37 ℃ by a temperature controller system (PTC10, Stanford Research Systems, USA). A magnetic stirrer along with a long magnetic bar (11-100-16S, Fisher Scientific, USA) was used to uniform the water temperature. A MATLAB-based program was developed to synchronize three different parts in the system, including ultrasound generation, camera exposure and HIFU transducer movement. The time sequence of the system is shown in *Figure 1B*. At each scanning point, the program controlled the camera to take an image with an exposure time of 1.5 s before the ultrasound exposure (i.e., heating) as a background used for signal processing. The FG2 then received a trigger from the MATLAB program in the computer through

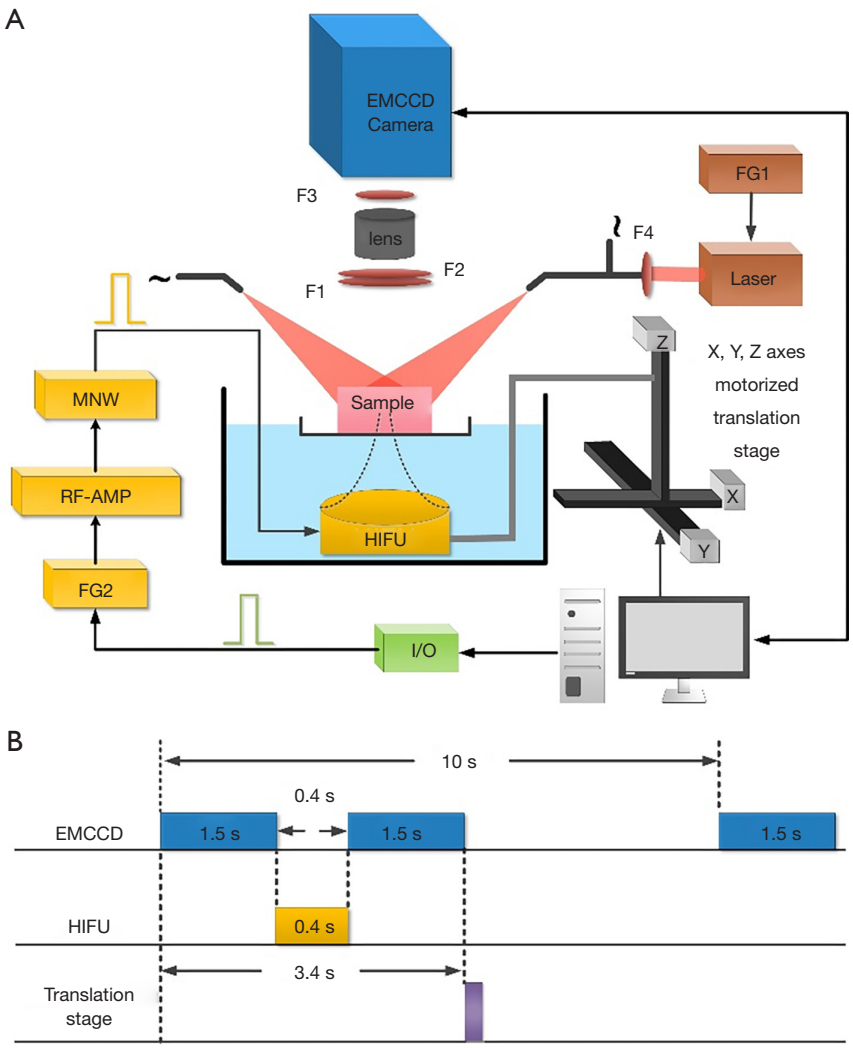

Figure 1 The schematic diagram (A) and the time sequence diagram (B) of the improved EMCCD-based USF imaging system. EMCCD, electron multiplying charge-coupled device; HIFU, high intensity focused ultrasound; MNW, matching network; RF-Amp, radio-frequency power amplifier; FG, function generator; I/O, multifunctional input/output device; F1-F3, emission filters (830 LP); F4, excitation filter (785/62 BP).

a multifunctional input/output device (I/O, PCIe-6363, National Instruments, USA), and generated a sinusoidal wave (frequency: 2.5 MHz, duration time: 0.4 s) to drive the HIFU transducer. Immediately after the ultrasound heating, another image with the same exposure time was acquired by the EMCCD camera. The increase of the fluorescence intensity between the two images was considered as the USF signal. After camera exposure, the MATLAB program controlled the translation stage to move the HIFU transducer to the next scanning point. To avoid the thermal diffusion-induced signal interference, the time interval between two adjacent scanning points was 10 s.

USF imaging of a sub-millimeter silicone tube embedded in chicken breast tissues

A sub-millimeter silicone tube (inner diameter: 0.76 mm, outer diameter: 1.65 mm, ST 60-011-04, Helix Medical, USA) was inserted into a piece of chicken breast tissue at a height of ~5 mm from the bottom surface to simulate a blood vessel. Since the thickness of a single piece of chicken breast tissue was limited (i.e., ≤3 cm), another one

(for thickness: 3.5, 4.5 or 5.0 cm) or two (for thickness: 5.5 cm) pieces of chicken breast tissue were stacked on the first one where the silicone tube was embedded to obtain the targeted thickness (Figure S1). The multiple-piece tissue was placed on a transparent parafilm (PM-992, BEMIS Company Inc., USA) that was used to seal an open window at the bottom center of a small plastic box. In order to maintain the ultrasound coupling, ultrasound gel (Aquasonic 100, Parker Laboratories Inc., USA) was used to fill the gap between the parafilm and the tissue. The top surface of the tissue was also covered by ultrasound gel and parafilm to keep it from drying out during the experiment. The USF contrast agents were injected into the silicone tube via a syringe. The silicone tube was washed after each experiment by injecting water and filled with new contrast agent solution for the next experiment. The bottom of the small plastic box was immersed into a water tank (water temperature: 37 ℃) to keep the USF contrast agents at body temperature. An area of 8.128 (X) × 4.064 (Y) mm^2 (step size in X direction: 0.2032 mm; in Y direction: 2.032 mm) was raster scanned by the ultrasound focus with an estimated ultrasound power of 1.74 W under various EM gains. The maximum applicable EM gain was limited by the dynamic range of the camera (0 to 65535 counts). The intensity of the excitation light illuminated on the tissue surface was 28.35 mW/cm^2 (Power: 20.10 mW, sensor's area: 0.709 cm^2) measured at the center of the illumination spot on the tissue surface via a photodiode power sensor (S120C, Thorlabs Inc., USA) and a power and energy meter (PM100D, Thorlabs Inc., USA).

The comparison of the EM gain stability between the external hardware trigger mode and the MATLAB trigger mode

The comparison of the external hardware trigger mode and the MATLAB trigger mode was realized in the same silicone tube embedded in 5.0 cm-thick chicken breast tissue. The silicone tube was filled with water during the experiment (i.e., the light source was tissue's autofluorescence, see analysis in Supplementary). Briefly, the only difference between the two trigger modes was the trigger source. All the parameters of the EMCCD camera (e.g., exposure time, number of frames, EM gain and trigger response) were set via the LightField software (Princeton Instruments, USA). In external hardware trigger mode, the trigger response was set as 'Start on a single trigger' which means the camera won't begin to take the images until the trigger circuit detected the rising edge of an external hardware trigger. In MATLAB trigger mode, the Lightfiled received commands from MATLAB via software interface (provided by the manufacturer) to control the camera to take the images. The trigger response was set as 'No response' which means the trigger circuit didn't work and the camera won't respond to the external hardware trigger. In this experiment, the camera exposure time of each frame image was 0.2 s and a total of 25 images were acquired continuously. The EM gain was set as various values (i.e., 1, 9, 27 or 81). All the other parameters of the Lightfield were set as default values.

Compare the ICG-liposome and the ICG-nanogel

The ICG-nanogel was synthesized according to the previously proposed protocol (20). To compare the ICG-nanogel with the ICG-liposome, the concentration of the initial ICG (i.e., the mass of the initial ICG divided by the volume of the final solution) was remained the same (0.016 mg/mL) by diluting the synthetized ICG-nanogel solution (0.056 mg/mL). The synthesized ICG-nanogel was tested by the in-house built fluorescence spectrometer with the same setting parameters used for the ICG-liposome. The comparison of USF imaging performance between the ICG-liposome and the ICG-nanogel were realized in the same silicone tube embedded in 2.5 cm-thick chicken breast tissue. The EM gain was set as 1 for both contrast agents.

Results

The ICG-liposome characterization

The details of characterization methods can be found in Supplementary. As shown in *Figure 2A*, the fluorescence intensity of the ICG-liposome increases with the rise of the solution temperature and the lower critical solution temperature (LCST) is 38.4 ℃ (defined as where the slope of the curve was 10% of its maximum value). The fluorescence intensity increases 2.02 folds when the temperature rises from 38.4 to 40.4 ℃. As shown in *Figure 2B*, the hydrodynamic size of the ICG-Liposome is 181.0±58.1 nm. The polydispersity is 0.126.

The comparison of the EM gain stability between the MATLAB trigger mode and the external hardware trigger mode

Figure 3A shows the first frame of the 25 images taken by

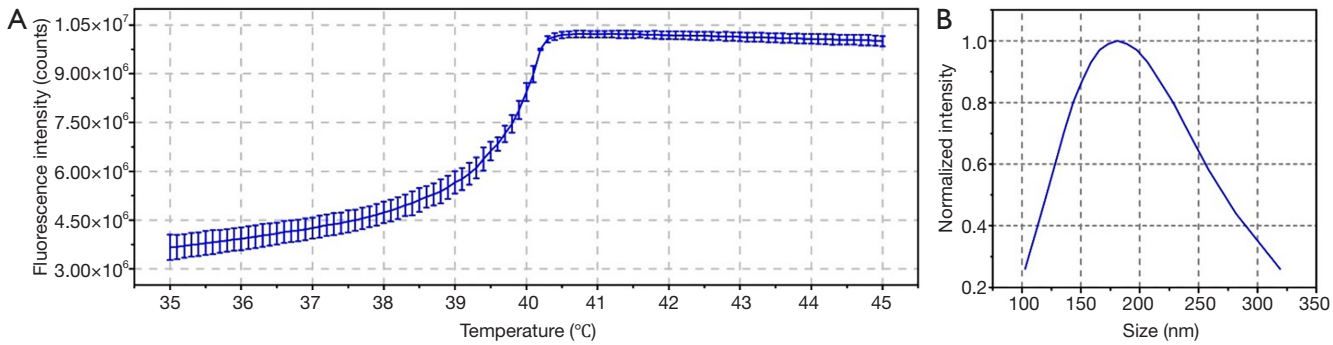

Figure 2 The characterization results of ICG-liposome. (A) The fluorescence intensity of ICG-liposome versus the solution temperature. (B) Hydrodynamic size of the synthesized ICG-liposome. ICG, indocyanine green.

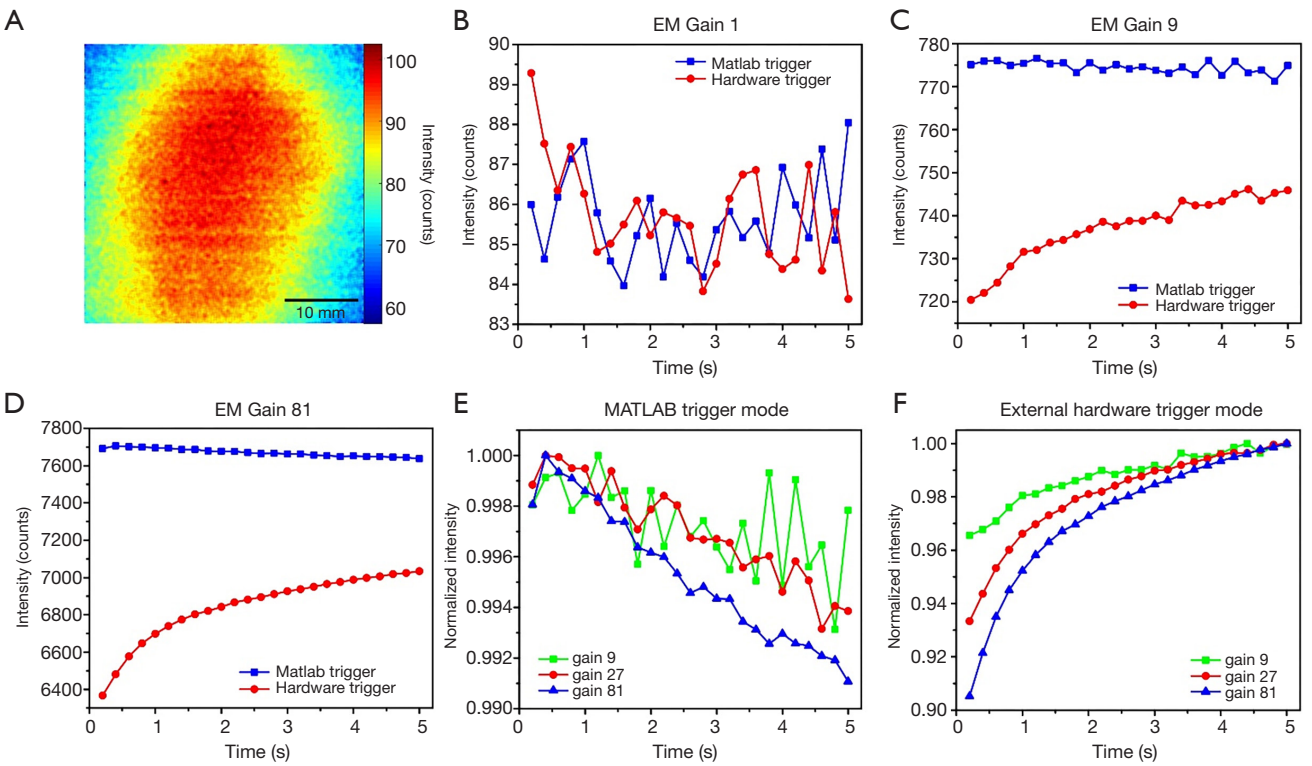

Figure 3 The comparison results of the MATLAB trigger mode and the external hardware trigger mode. (A) The first frame of the images taken by the camera with an EM gain of 1 in MATLAB trigger mode. The mean intensity of the acquired 25 frames in MATLAB trigger mode (blue line with squares) and external hardware trigger mode (red line with circles) with an EM gain of (B) 1, (C) 9 and (D) 81. Normalized mean intensity curve using (E) MATLAB trigger mode and (F) external hardware trigger mode with an EM gain of 9 (green line with squares), 27 (red line with circles), and 81 (blue line with triangles). EM, electron multiplying.

the EMCCD camera with an EM gain of 1 in MATLAB trigger mode. *Figure 3B,C,D* show the mean intensity (i.e., spatial average value of the whole 2D fluorescence image) of the acquired 25 frames using MATLAB trigger mode (blue line with squares) and the hardware trigger mode (red line with circles) with an EM gain of 1, 9 and 81, respectively. As shown in *Figure 3B*, the mean intensities of the two modes are fluctuated and similar to each other when the EM gain

is 1. As shown in *Figure 3C,D*, the mean intensity of the MATLAB trigger mode is higher and more stable than that of the external hardware trigger mode with an EM gain of 9 or 81. The curve of the hardware trigger mode continuously rises with a higher increase rate at the beginning. *Figure 3E* shows the normalized mean intensity using the MATLAB trigger mode with an EM gain of 9 (green line with squares), 27 (red line with circles), and 81 (blue line with triangles). The maximum decrease of the mean intensity is less than 1% and the higher EM gain leads to slightly more intensity decrease. However, when using external hardware trigger mode (*Figure 3F*), the maximum increase of the mean intensity can reach as high as ~10% and the higher EM gain leads to a higher intensity increase.

USF imaging of the sub-millimeter silicone tube embedded in chicken breast tissue

All the signals shown on a 2D-USF-signal image (Figure S2) are generated from USF photons and induced by the ultrasound focus at a specific scan point. We average these signals to form a single value to represent the USF signal at this specific scan point of the ultrasound focus. By scanning the ultrasound focus on the X-Y 2D plane, we can form a 2D USF image. *Figure 4A* shows the 2D USF images of the sub-millimeter silicone tube with an EM gain of 1, 3, 9, 27 and 54 in the 4.5 cm-thick chicken breast tissue. The image of the silicone tube is very noisy with the EM gain of 1. When increasing of the gain from 1 to 9, the image becomes much clearer. However, further increasing the gain from 9 to 54, the quality of images remains similar. The SNR values (see calculation method in Supplementary, Figure S3) are 10.69±1.39, 14.88±1.39, 23.52±2.96, 21.7±0.64 and 20.88±0.35 dB corresponding to the EM gain of 1, 3, 9, 27 and 54, respectively. Obviously, by optimizing the EM gain, we can significantly improve the SNR of a USF image. By adopting the optimized EM gain, *Figure 4B* shows the USF images of the silicone tube in the different thick chicken breast tissues (2.5 cm: EM gain 3; 3.5, 4.5 and 5.0 cm: EM gain 9; 5.5 cm: EM gain 54). The SNR values are 41.56±1.96, 37.45±3.75, 23.53±2.96, 12.78±2.07 and 8.69±1.46 dB corresponding to the thickness of 2.5, 3.5, 4.5, 5.0 and 5.5 cm, respectively. Although the SNR still decreases with the increase of tissue thickness, the decrease of image quality slows down because the SNR at deeper tissue is improved by the optimized EM gain. *Figure 4C* shows the SNR of the USF images versus the EM gain in different thick tissues. The SNR increases quickly when the EM gain rises from 1 to 9 (thickness: 2.5, 3.5, 4.5 and 5.0 cm) and then reduces slightly or remains stable when the EM gain rises from 9 to 54 (thickness: 4.5 and 5.0 cm). *Figure 4D* shows the USF signal and the noise versus the EM gain for the 4.5 cm- and 5.0 cm-thick tissue samples. In both thicknesses, the USF signal shows a higher increase rate than the noise in the gain range of 1–9. However, after gain is >9, both the signal and the noise show a similar increase rate versus the gain, which explains why the SNR becomes flat when gain is >9. *Figure 4E* shows the full width at half maximum (FWHM) of the USF images of the silicone tube in different thick tissues. They are closed to the outer diameter of the silicone tube (i.e., 1.65 mm). Ideally, the FWHM is mainly determined by the convolution of the ultrasound or thermal focal size (the lateral FWHM of the acoustic intensity focus is 0.55 mm) with the object size, and should be independent of tissue's thickness. The slight increase of the FWHMs in *Figure 4E* may be because of the fact that the USF images become much noisier in deeper tissue and the estimated FWHMs are less accurate than those in shallower tissue.

The comparison between the ICG-liposome and the ICG-nanogel

Figure 5A shows the fluorescence intensity as a function of the temperature of the sample solution (ICG-liposome: red line with circles; ICG-nanogel: blue line with squares). The fluorescence increase of the ICG-liposome is much sharper than that of the ICG-nanogel. As mentioned in *Figure 2A*, the fluorescence increases 2.02 folds in a narrow temperature range of 2.0 ℃ (i.e., from 38.4 to 40.4 ℃). The ICG-nanogel shows a LCST at 35.1 ℃ and the fluorescence increases 2.74 folds in a relatively wide temperature range of 7.4 ℃ (i.e., from 35.1 to 42.5 ℃). Although the investigation of the mechanism why the ICG-liposome has a sharper temperature switching curve is out of the scope of this study, it may be related to the capability of the material response to temperature and should be investigated in future. In addition, the increase of the absolute fluorescence intensity of the ICG-liposome was 3.0 times stronger than that of ICG-nanogel (i.e., 5.12e6 counts versus 1.69e6 counts), which may be caused by the higher ICG encapsulating efficiency of ICG-liposome with the same initial ICG concentration. A stronger increase in the absolute fluorescence intensity ($\Delta I_{On-Off}=I_{On}-I_{Off}$) within

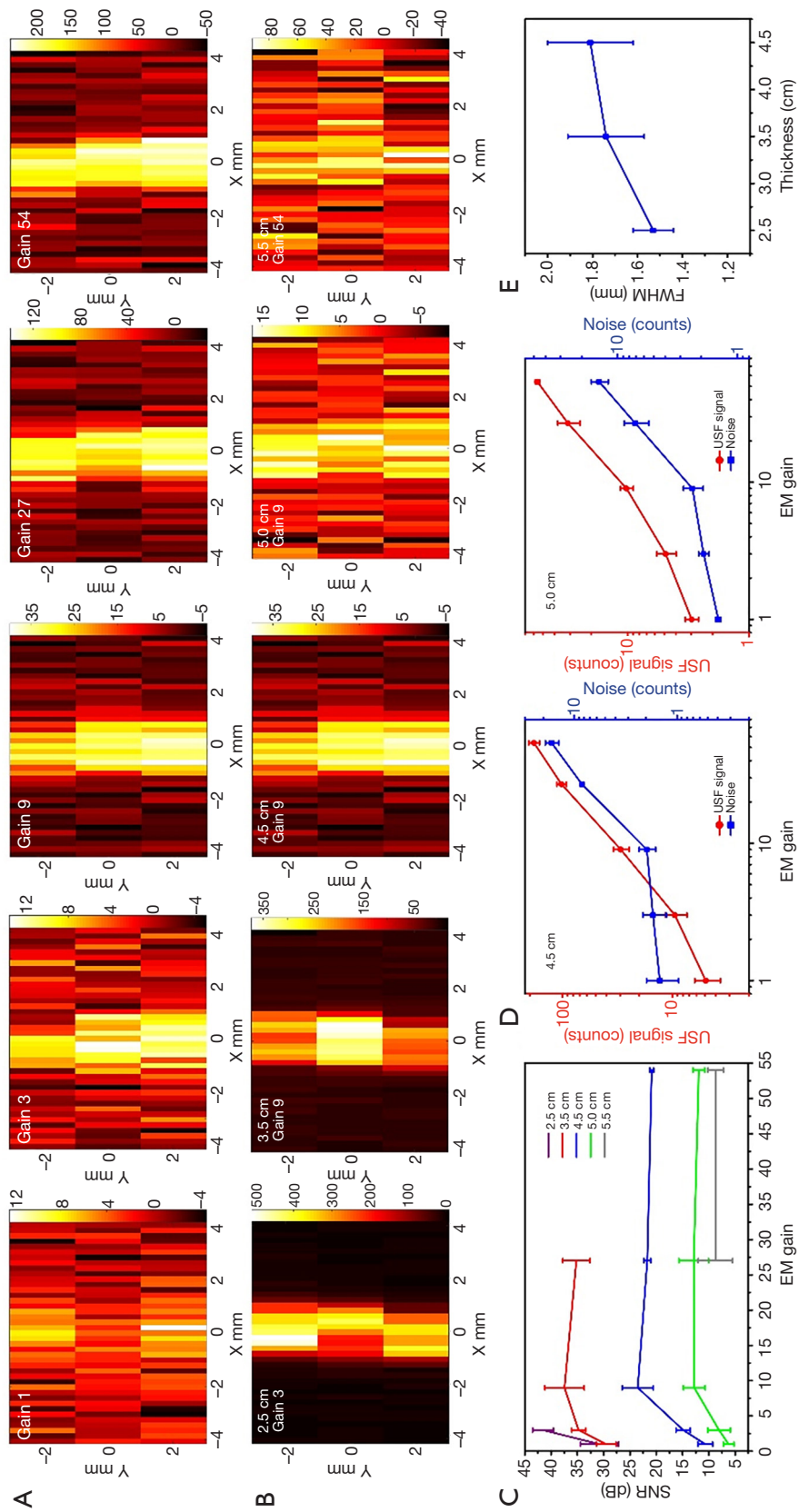

Figure 4 The USF imaging results in different thick tissues with various EM gains. (A) The USF images of the silicone tube in the 4.5 cm-thick chicken breast tissue with different EM gains of 1, 3, 9, 27 and 54, respectively. (B) The USF images of the silicone tube in the chicken breast tissue with different thicknesses of 2.5, 3.5, 4.5, 5.0 and 5.5 cm, and with an EM gain of 3, 9, 9, 9 and 54, respectively. (C) The SNR of the USF images with different EM gains in various thick tissue (2.5 cm: purple line; 3.5 cm: red line; 4.5 cm: blue line; 5.0 cm: green line; 5.5 cm: grey line). (D) The average intensity of USF signal (red line with circles) and the average noise (blue line with squares) with different EM gains in 4.5 cm-thick tissue and 5.0 cm-thick tissue. (E) The FWHM of the USF image of the silicone tube with different thicknesses (2.5 cm: EM gain 3; 3.5 cm: EM gain 9; 4.5 cm: EM gain 9). USF, ultrasound-switchable fluorescence; EM, electron multiplying; SNR, signal-to-noise ratio; FWHM, full width at half maximum.

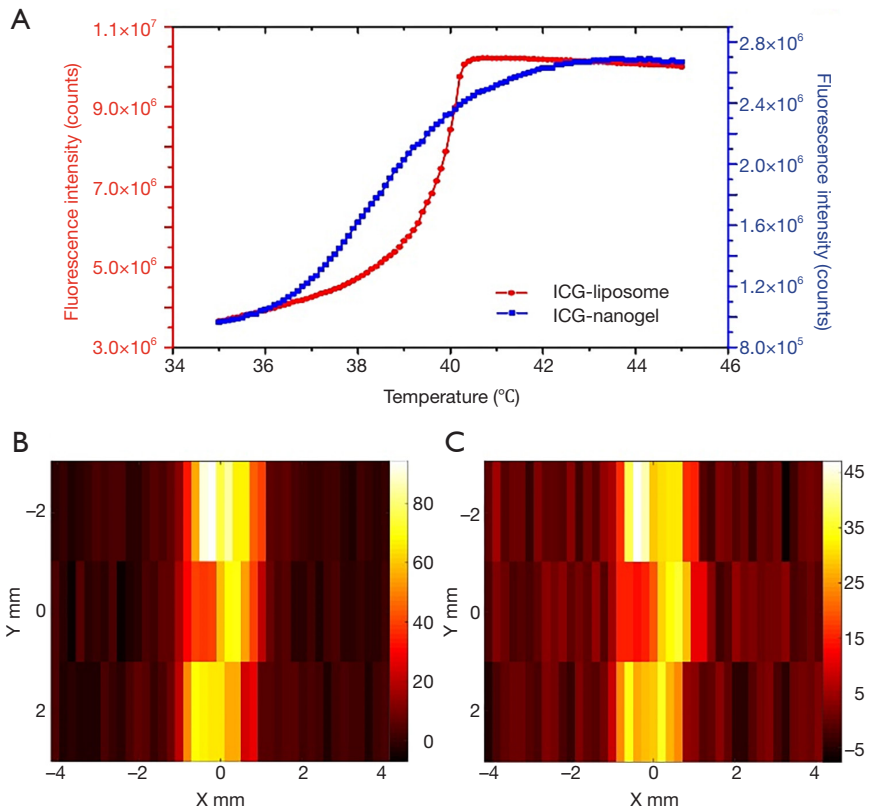

Figure 5 The comparison results of ICG-liposome and ICG-nanogel. (A) The fluorescence intensity of the ICG-liposome (the red line with circles) and the ICG-nanogel (the blue line with squares) versus temperature. The USF image of the silicone tube filled with ICG-liposome (B) and ICG-nanogel (C) in 2.5 cm-thick chicken breast tissue with an EM gain of 1. All experiment parameters were same. USF, ultrasound-switchable fluorescence; ICG, indocyanine green; EM, electron multiplying.

a narrower temperature range ($\Delta T_{On-Off}=T_{On}-T_{Off}$) indicates a higher (absolute) temperature sensitivity of the contrast agent (i.e., $S_{abs}=\Delta I_{On-Off}/\Delta T_{On-Off}$), which has a unit of counts per ℃. The S_{abs} of the ICG-liposome and ICG-nanogel are 2.56e6 counts/℃ and 0.23e6 counts/℃, respectively. The higher temperature sensitivity of the contrast agent will be favorable for USF imaging to achieve a higher SNR because it will provide more USF photons using the same ultrasound/thermal energy. This speculation is verified in *Figure 5B,C* in which the SNR of the USF image of the silicone tube filled with the ICG-liposome (*Figure 5B*) and ICG-nanogel (*Figure 5C*) is 30.79±3.61 and 26.34±2.03 dB, respectively (note that the tissue thickness is 2.5 cm and the EM gain is 1, and all other experimental parameters remained the same). Therefore, the ICG-liposome has a better USF performance than the ICG-nanogel because of its higher temperature sensitivity.

Discussion

In current study, we demonstrated that improving the sensitivity of both the USF contrast agent and the imaging system could significantly increase the SNR of USF imaging. The USF imaging of a silicone tube in a 5.5 cm-thick (i.e., 5.0 cm deep from the top) chicken breast tissue with an illumination intensity of 28.35 mW/cm^2 was successfully demonstrated (*Figure 4B*) via two key factors: (I) the USF contrast agent with high temperature sensitivity; (II) the USF imaging system with high detection sensitivity.

In our previous studies, we usually defined a fluorescence on-to-off ratio of the USF contrast agent ($R_{On/Off}=I_{On}/I_{Off}$) as a parameter to characterize the contrast agent's USF performance (15,19). Recently, we reported that this ratio was an effective parameter only when the background photons (i.e., the autofluorescence and laser leakage) are

significantly less than the background fluorescence photons generated from the non-100%-off contrast agent (21). This is usually happening in shallow-tissue USF imaging (such as at a depth of <2–3 cm). When imaging deep tissue (such as >3 cm) or the USF contrast agent has a very low quantum efficiency at the off state, the background fluorescence photons are much weaker than or comparable to the background photons (Figure S1). In this situation, the $R_{On/Off}$ is less effective to characterize the contrast agent's USF performance. Instead, the on-and-off difference of the absolute fluorescence intensity (ΔI_{On-Off}) becomes a good indicator for the USF contrast agent if other parameters remain the same. In addition, we also moved one more step further to define the (absolute) temperature sensitivity of a USF contrast agent ($S_{abs}=\Delta I_{On-Off}/\Delta T_{On-Off}$) after comparing the two types of contrast agents, ICG-liposomes versus ICG-nanogels. Obviously, a contrast agent with high (absolute) temperature sensitivity should provide a high SNR in USF imaging, which has been demonstrated in *Figure 5*.

It is important to point out that the noise of the USF imaging is different from the noise of the 2D planar fluorescence imaging via an EMCCD camera. In 2D planar fluorescence imaging, the main noise components are photon shot noise, dark current noise, clock induced charge noise and readout noise (22). These noise electrons directly affect each pixel of the image taken by the camera. However, the noise of the USF imaging is the variation of the difference of the mean spatial intensities between two sequential images taken by the camera when ultrasound is off. In an ideal situation, this difference of the mean spatial intensities should be zero or an invariable value. According to the definition of the USF image's noise (see details in supplementary), the noise would be zero in this ideal situation. Unfortunately, the difference in a real case is variable because of various reasons, such as the excitation light, bias of the camera and/or the variation of the EM gain, and others, which are unstable and dependent on environment.

In this study, we focused on: (I) the method to stabilize the EM gain; (II) the affection of the EM gain on USF image's quality while all other parameters kept the same. The EM gain is more stable in MATLAB trigger mode than the external hardware trigger mode (*Figure 3*). The reason may be the larger environment temperature change inside the camera while waiting for an external hardware trigger. The higher environment temperature inside the camera may reduce the probability of charge multiplication and therefore lower the EM gain under the same voltage applied across the multiplication register (23). It's interesting to find that the changes of the mean intensity curves are opposite in these two modes. The temperature of the sensor is kept at −55 ℃ (default value) through thermoelectric cooling with an internal fan. However, the real temperature may be above this value when the circuit is working (e.g., waiting for the external trigger or taking images). New thermal equilibrium would be reached at a temperature (T1: taking images; T2: waiting for the external trigger; T1 < T2) lower than −55 ℃. Thus, the spatial mean intensity decreases (*Figure 3E*)/increases (*Figure 3F*) when the generated thermal energy is more/less than that taken away by the cooling system. Although we may not be able to conclude that the issue of the gain stability under different triggering modes is a common problem for all EMCCD cameras (because we do not have access to other types), we have tested two EMCCD cameras with the same model (i.e., ProEM®-HS:1024BX3) in this study and found the similar results. Therefore, we can conclude that this issue is not a defect of a specific camera.

The noise increases much slower than the USF signal when the EM gain rises from 1 to 9, and follows a similar increase as the USF signal when the EM gain is larger than 9 (*Figure 4D*). As mentioned above, the change of the USF imaging's noise is coming from the change of the stability of the EM gain because all other parameters are same. The EM gain seems to be more stable when the gain is low (<9). Thus, rising the EM gain (<9 in this study) helps to improve the SNR of the USF image in a tissue with a thickness less than 5.5 cm (*Figure 4C*). It should be noted that the USF imaging system reaches its detection limitation in 5.5 cm-thick chicken breast tissue with current setting so that the quantitative analysis may not reliable. The silicone tube can only be roughly differentiated with an EM gain of 54, although the SNRs of with the EM gain of 27 and 54 are similar (Figure S4). Lastly, it should be mentioned that current study aims to demonstrate a general concept that the SNR in USF imaging can be improved by optimizing the EMCCD's gain. However, because we have not investigated other types of EMCCD cameras, cautions should be taken when extending the specific numbers provided here into other studies (such as the optimized gain of 9) because the numbers may vary among different cameras.

Conclusions

In this study, we successfully achieved USF imaging of a

sub-millimeter silicone tube (inner diameter: 0.76 mm, outer diameter: 1.65 mm) embedded in centimeter-deep chicken breast tissue (2.5, 3.5, 4.5, 5.0 and 5.5 cm) using a low intensity excitation light (28.35 mW/cm^2). The SNR improving strategies include (I) adopting a new contrast agent, ICG-liposome, with high USF performance and (II) stabilizing and optimizing the EM gain in the USF imaging system via a software trigger mode. The ICG-liposome showed better USF performance than the previous ICG-nanogel in deep tissue. The gain of the EMCCD camera used in the USF imaging system was stabilized by using the MATLAB trigger mode instead of the external hardware trigger mode. In conclusion, USF imaging can achieve high sensitivity (SNR) and high spatial resolution in several centimeters deep tissues using a low-intensity NIR-I excitation laser. With these unique features, it has dramatic potentials for different biomedical applications in future.

Acknowledgments

Funding: This work was supported in part by funding from the CPRIT RP170564 (Baohong Yuan).

Footnote

Provenance and Peer Review: With the arrangement by the Guest Editors and the editorial office, this article has been reviewed by external peers.

Conflicts of Interest: All authors have completed the ICMJE uniform disclosure form (available at http://dx.doi.org/10.21037/qims-20-796). The special issue "Advanced Optical Imaging in Biomedicine" was commissioned by the editorial office without any funding or sponsorship. All authors report grants from Cancer Prevention & Research Institute of Texas, during the conduct of the study. TY has a patent Systems and Methods for Thermometry and Theranostic Applications pending, a patent Ultrasound-switchable fluorescence imaging having improved imaging speed pending, and a patent significantly improving sensitivity of ultrasound-switchable fluorescence technique for high-resolution, deep tissue, and dynamic imaging pending. YL has a patent significantly improving sensitivity of ultrasound-switchable fluorescence technique for high-resolution, deep tissue, and dynamic imaging pending. BY has a patent Systems and Methods for high-resolution imaging issued, a patent Systems and Methods for Thermometry and Theranostic Applications pending, a patent Highly specific tissue imaging pending, a patent Multiple biomarkers imaging for high specificity pending, a patent Ultrasound-switchable fluorescence imaging having improved imaging speed pending, a patent Systems and Methods for surgical guidance in breast cancer surgery and lymph node dissection pending, and a patent significantly improving sensitivity of ultrasound-switchable fluorescence technique for high-resolution, deep tissue, and dynamic imaging pending.

References

1. Antaris AL, Chen H, Cheng K, Sun Y, Hong G, Qu C, Diao S, Deng Z, Hu X, Zhang B, Zhang X. A small-molecule dye for NIR-II imaging. Nat Materials 2016;15:235-42.
2. Wan H, Yue J, Zhu S, Uno T, Zhang X, Yang Q, Yu K, Hong G, Wang J, Li L, Ma Z. A bright organic NIR-II nanofluorophore for three-dimensional imaging into biological tissues. Nat Commun 2018;9:1171.
3. Chen G, Shen J, Ohulchanskyy TY, Patel NJ, Kutikov A, Li Z, Song J, Pandey RK, Ågren H, Prasad PN, Han G. (α-NaYbF4: Tm3+)/CaF2 core/shell nanoparticles with efficient near-infrared to near-infrared upconversion for high-contrast deep tissue bioimaging. ACS Nano 2012;6:8280-7.
4. Dang X, Bardhan NM, Qi J, Gu L, Eze NA, Lin CW, Kataria S, Hammond PT, Belcher AM. Deep-tissue optical imaging of near cellular-sized features. Sci Rep 2019;9:3873.
5. Si K, Fiolka R, Cui M. Fluorescence imaging beyond the ballistic regime by ultrasound-pulse-guided digital phase conjugation. Nat Photonics 2012;6:657.
6. Yuan B. Diffuse optical tomography and fluorescence diffuse optical tomography. Dissertation, University of Connecticut, January 2006.
7. Kobayashi M, Mizumoto T, Shibuya Y, Enomoto M, Takeda M. Fluorescence tomography in turbid media

based on acousto-optic modulation imaging. Appl Phys Lett 2006;89:181102.
8. Yuan B, Gamelin J, Zhu Q. Mechanisms of the ultrasonic modulation of fluorescence in turbid media. J Appl Phys 2008;104:103102.
9. Yuan B. Ultrasound-modulated fluorescence based on a fluorophore-quencher-labeled microbubble system. J Biomed Opt 2009;14:024043.
10. Yuan B, Liu Y, Mehl PM, Vignola J. Microbubble-enhanced ultrasound-modulated fluorescence in a turbid medium. Appl Phys Lett 2009;95:181113.
11. Lin Y, Kwong TC, Gulsen G, Bolisay L. Temperature-modulated fluorescence tomography based on both concentration and lifetime contrast. J Biomed Opt 2012;17:056007.
12. Kwong TC, Nouizi F, Lin Y, Cho J, Zhu Y, Sampathkumaran U, Gulsen G. Experimental evaluation of the resolution and quantitative accuracy of temperature-modulated fluorescence tomography. Appl Opt 2017;56:521-9.
13. Yuan B, Uchiyama S, Liu Y, Nguyen KT, Alexandrakis G. High-resolution imaging in a deep turbid medium based on an ultrasound-switchable fluorescence technique. Appl Phys Lett 2012;101:33703.
14. Pei Y, Wei MY, Cheng B, Liu Y, Xie Z, Nguyen K, Yuan B. High resolution imaging beyond the acoustic diffraction limit in deep tissue via ultrasound-switchable NIR fluorescence. Sci Rep 2014;4:4690.
15. Cheng B, Bandi V, Wei MY, Pei Y, D'Souza F, Nguyen KT, Hong Y, Yuan B. High-resolution ultrasound-switchable fluorescence imaging in centimeter-deep tissue phantoms with high signal-to-noise ratio and high sensitivity via novel contrast agents. PLoS One 2016;11:e0165963.
16. Kandukuri J, Yu S, Yao T, Yuan B. Modulation of ultrasound-switchable fluorescence for improving signal-to-noise ratio. J Biomed Opt 2017;22:76021.
17. Yao T, Yu S, Liu Y, Yuan B. Ultrasound-switchable fluorescence imaging via an EMCCD camera and a Z-scan method. IEEE Journal of Selected Topics in Quantum Electronics 2018;25:1-8.
18. Yao T, Yu S, Liu Y, Yuan B. In vivo ultrasound-switchable fluorescence imaging. Sci Rep 2019;9:9855.
19. Yu S, Cheng B, Yao T, Xu C, Nguyen KT, Hong Y, Yuan B. New generation ICG-based contrast agents for ultrasound-switchable fluorescence imaging. Sci Rep 2016;6:35942.
20. Liu R, Yao T, Liu Y, Yu S, Ren L, Hong Y, Nguyen KT, Yuan B. Temperature-sensitive polymeric nanogels encapsulating with β-cyclodextrin and ICG complex for high-resolution deep-tissue ultrasound-switchable fluorescence imaging. Nano Res 2020;1:1-1.
21. Liu Y, Yao T, Cai W, Yu S, Hong Y, Nguyen KT, Yuan B. A Biocompatible and Near-Infrared Liposome for In Vivo Ultrasound-Switchable Fluorescence Imaging. Adv Healthc Mater 2020;9:e1901457.
22. Zhang WW, Chen Q, Zhou BB, He WJ. Signal-to-Noise Ratio Improvement of EMCCD Cameras. World Academy of Science, Engineering and Technology 2010;4:966-70.
23. Ingley R, Smith DR, Holland AD. Life testing of EMCCD gain characteristics. Nuclear Instruments and Methods in Physics Research Section A: Accelerators, Spectrometers, Detectors and Associated Equipment 2009;600:460-5.

Cite this article as: Yao T, Liu Y, Ren L, Yuan B. Improving sensitivity and imaging depth of ultrasound-switchable fluorescence via an EMCCD-gain-controlled system and a liposome-based contrast agent. Quant Imaging Med Surg 2021;11(3):957-968. doi: 10.21037/qims-20-796